$$k_x \frac{\partial^2 P}{\partial x_A^2} + k_y \frac{\partial^2 P}{\partial y_A^2} = 0 \qquad (2)$$

with the boundary condition that the gradient of pressure is zero on all the boundaries except at the source at (x_A', B) and at the sink at $(x_A'', 0)$, where we have constant input and output, respectively. The solution to this boundary value problem was already given in reference *1*.

Pressure drop measurements were made at various points on an actual Allis-Chalmers hydrogen plate as shown in Figure 3. The pressure drop vs. flow rate relationships between the different points of measurement are shown in Figure 2. The pressure profile generated along $x = 0.05$ was matched against a theoretical profile, and the results are graphically presented in Figure 3. It should be noted that, in order to plot each experimental point shown in Figure 3, it was necessary to generate a complete flow rate vs. pressure drop profile as shown in Figure 2. The maximum deviation between the experimental and theoretical values is ±5%. An error of this magniutde is conceivable on the basis of errors in pressure drop, flow rate readings, and volume of gas in the chambers. This verification enables us to use Darcy's law for description of fluid motion in fuel cell cavities with confidence.

ACKNOWLEDGMENT

This study was supported by the National Aeronautics and Space Administration under Contract No. NAS8-21159. The authors thank Professor Charles Tobias for a useful discussion of this problem.

NOTATION

a = dimensionless width of plate, $A/B\sqrt{k_y/k_x}$
A = width of plate, ft.
B = length of plate, ft.
k_x, k_y = permeabilities in the x_A and y_A directions respectively, ft.^{2}
L = distance between points for pressure drop measurement, ft.
P = pressure, lb.$_f$/sq.ft.
ΔP = pressure drop, mm. Hg.
$\overline{P}$ = dimensionless pressure drop, $\dfrac{\Delta P g_c V_g \sqrt{k_x k_y}}{QAB\mu}$
Q = volumetric flow rate, cu.ft./sec.
V_g = volume of fluid in gas compartment, cu.ft.
W = mass flow rate, lb.$_m$/hr.
x = dimensionless space coordinate, $(x_A/B)\sqrt{k_y/k_x}$
x_A = actual space coordinate, ft.
y_A = actual space coordinate, ft.
μ = viscosity, lb.$_m$/ft.-sec.
ρ = density, lb.$_m$/cu.ft.

LITERATURE CITED

1. Gidaspow, Dimitri, and Sareen, S. S., *AIChE J.*, **16**, 560-568 (1970).
2. Lyczkowski, R. W., and Gidaspow, D., paper presented at the 20th Comite Intern. Thermodyn. Cinet. Electrochim. meeting, Strasbourg, France (September 15-20, 1969). Extended Abstracts, pp. 431-434. Accepted for publication in the AIChE J., August 24, 1970.
3. Sareen, S. S., Ph.D. thesis, Illinois Inst. Technol., Chicago (1970).

Note on the Feedback Control of a Stirred Tank Reactor

GAYLORD G. GREENFIELD and THOMAS J. WARD

Chemical Engineering Department
Clarkson College of Technology, Potsdam, New York 13676

Huber and Kermode (*1*) recently presented a "predictive feedback" regulator control analysis for linear, lumped, single-variable process systems containing time delays and a sample-hold combination. Some additional insight into this regulator scheme can be obtained from an analysis of the information flow in the system. The process model used by these authors can be represented by the signal flow diagram of Figure 1. Conventional feedback control of this process is shown by the dashed line of Figure 2, which corresponds to Figure 1 of the cited reference.

PROPOSED CONTROL SCHEME

In the method proposed by Huber and Kermode, two more control functions are added to reduce the effects of the operator D on the control quality. This control scheme is illustrated in Figure 3, where the two controllers are shown as F_1 and F_2. This Figure 3 corresponds to Figure 4 of the cited reference. The controller F_1 is specified as the negative of the transmission path $(g_1/g_2)D$ from $\hat{\theta}$ to $\hat{x}^*$. This exactly eliminates the transmission from $\hat{\theta}$ to $\hat{x}^*$. The controller F_2 is then specified as being equal to the

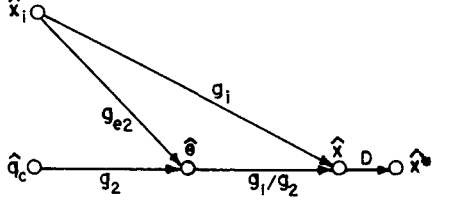

Fig. 1. Continuous flow stirred tank reactor model.

Correspondence concerning this communication should be addressed to Prof. Thomas J. Ward. Gaylord G. Greenfield is with Continental Oil Co., Ponca City, Oklahoma 74601.

transmission path (g_1/g_2) from $\hat{\theta}$ to $\hat{x}$.

In other words, these two control functions effectively cancel the transmission between $\hat{\theta}$ and $\hat{x}$. The result corresponds to Figure 4. Note that the variable $\hat{f}_{10}$ is not equal to $\hat{x}$ or $\hat{x}^*$. Rather, $\hat{f}_{10} = (g_1/g_2)\hat{\theta} + g_i D\hat{x}_i$, a function of the present temperature and the delayed, sampled inlet composition. The present and the sampled, delayed reactor composition ($\hat{x}$ and $\hat{x}^*$) have both, in effect, been eliminated from the controlled system.

The information flow represented in Figure 4 can also be shown as in Figure 5. The significance of the proposed control scheme is more evident if Figure 5 is then drawn as shown in Figure 6. This illustration clearly shows that the proposed control scheme consists of feedback control of the reactor temperature $\hat{\theta}$ and feedforward control of the inlet composition disturbance $\hat{x}_i$. The reactor composition $\hat{x}$ is not directly regulated at all. Figure 6 also shows clearly why the characteristic equation of the controlled system does not contain the operator D.

Three additional items should be noted with regard to the proposed scheme:

1. The use of different g_c functions in the two controller paths of Figure 6 would give better results for the problem simulated.
2. The effect of D in the feedforward path of Figure 6 is analogous to model error in the ideal single-variable feedforward-feedback control problem. The desirability of using feedforward control will depend on the amount of model error introduced into the ideal model structure by the operator D. This problem has been thoroughly treated by Luecke and McGuire (2).
3. Because the reactor composition is not actually regulated in the proposed scheme, more effective use of the composition analyzer could be obtained by using it to measure the inlet composition $\hat{x}_i$ directly. This would eliminate both g_i from the feedforward path of Figure 6 and the need for the controller F_1.

DESIGN PROCEDURE

The application of these three items to the feedback temperature control and feedforward disturbance control of Figure 6 would lead to Figure 7. Here G_C is the feedback controller and G_F is the feedforward controller. An effective, simple design procedure would be as follows:

1. Determine G_F from the invariance principle, ignoring the operator D in the feedforward path. Approximate the resulting G_F function as closely as desirable.
2. Use standard single-variable feedback design procedures to design G_C.

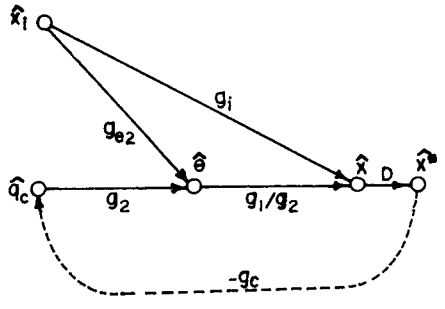

Fig. 2. Conventional feedback control of the reactor.

3. Select the arbitrary weighting constant W. This constant allocates the control effort between the feedforward and feedback roles. It would depend on both the relative model error introduced by the analyzer dynamics D and the approximation made in G_F above. In this reactor ex-

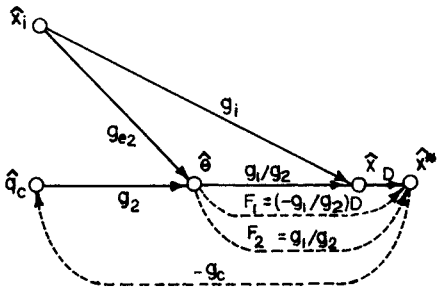

Fig. 3. "Predictive feedback control" of the reactor.

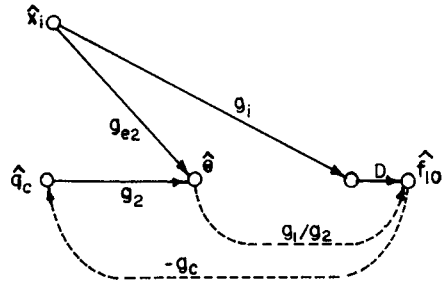

Fig. 4. Effective controlled system.

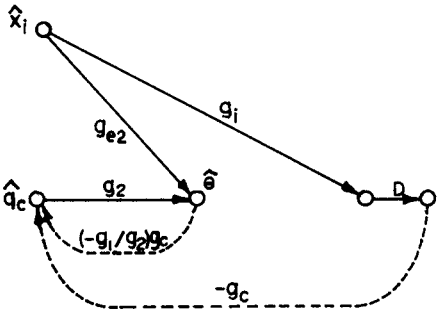

Fig. 5. An equivalent structure of the effective control.

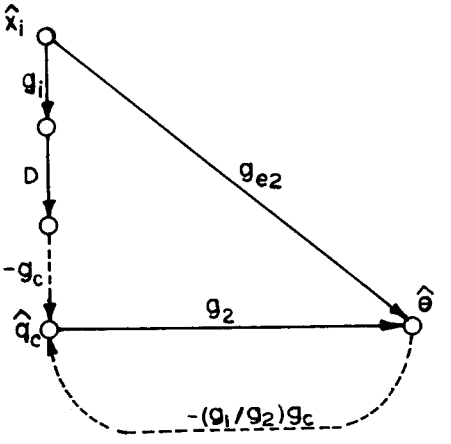

Fig. 6. Basic controller functions of "predictive feedback."

ample, the best value of W would probably be less than one and possibly even zero.

This "near-optimal" procedure is based on the optimal composite feedforward-feedback control study of Luecke and McGuire (2). The same method could be applied to Figure 6 if the inlet composition were actually not available for measurement. If the total control effort available is limited by manipulative input constraints, the constraints can be included directly (as in saturation clipping) or treated in terms of a penalty function.

In this note, a straightforward signal flow graph analysis has provided valuable insight into an involved multiloop control scheme. It is an example of the value of graphical signal flow diagrams as analytical aids in control system design.

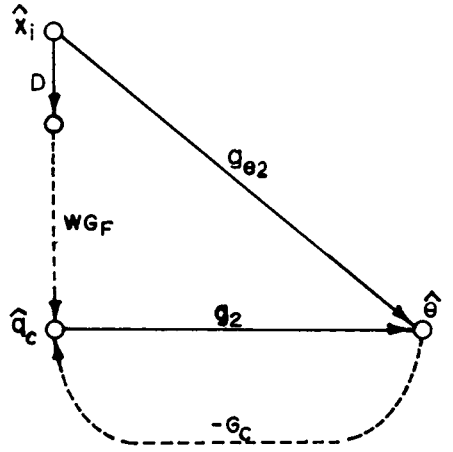

Fig. 7. Feedback temperature-feedforward disturbance control.

ACKNOWLEDGMENT

This analysis was partially supported by the National Science Foundation Grant GK-3735.

NOTATION

Λ = Laplace transform of the variable perturbation from steady state
D = operator representing the time delays L_1 and L_2, the sampler T_1, and zero-order hold h_1 of reference (1)
f_{10} = a variable generated by the controlled process system
F_1 = a controller function of the predictive-feedback scheme
F_2 = a controller function of the predictive-feedback scheme
g_c = a controller function of the predictive-feedback scheme
g_1, g_2, g_3, g_{e2} = process transfer functions given in reference (1)
G_C = a feedback controller function
G_F = a feedforward controller function
q_c = coolant flow rate
w = weighting constant of composite feedforward-feedback control
x = reactor composition variable
x^* = delayed, sampled reactor composition variable
x_i = inlet composition variable
θ = reactor temperature

LITERATURE CITED

1. Huber, C. I., and Kermode, R. I., *AIChE Journal*, 16, 6, 911 (Nov. 1970).
2. Luecke, R. H., and McGuire, M. L., *AIChE Journal*, 14, 1, 181 (1968).

Comments on "A Phenomenological Interpretation and Correlation of Drag Reduction"

R. J. GORDON

Department of Chemical Engineering
University of Florida, Gainesville, Florida 32601

In the above-mentioned paper (1), Astarita, Greco, and Nicodemo proposed the following correlation for turbulent drag reduction in dilute polymer solutions:

$$\frac{f}{f_0} = \beta\,(N_{De}) \qquad (1)$$

Here f is the measured friction factor, f_0 the friction factor predicted from the usual Newtonian relationship (2), and $N_{De} = \theta\ U/D\ N_{Re}^{0.75}$ is the Deborah number (1). In the development of Equation (1), it was assumed that θ, the characteristic fluid time, is constant for a given polymer solution.

According to the aforementioned authors, $\beta(N_{De})$ should be a universal function; that is, independent of solution characteristics, Reynolds number, and tube diameter. This being the case, Equation (1) may be rewritten as

$$\frac{f}{f_0} = \beta\left(\frac{N_{De}}{N_{De,0.5}}\,N_{De,0.5}\right)$$

where $N_{De,0.5}$ is the unique Deborah number corresponding to $\beta = 0.5$. It follows that

$$\frac{f}{f_0} = \beta\left[\frac{\frac{U}{D}N_{Re}^{0.75}}{\left(\frac{U}{D}N_{Re}^{0.75}\right)_{,0.5}}\,N_{De,0.5}\right] = \beta'\left(\frac{\omega}{\omega_{,0.5}}\right) \qquad (2)$$

where $\omega = U/D\ N_{Re}^{0.75}$ is a characteristic frequency.

Astarita and his co-workers verified Equation (2) by plotting f/f_0 versus $\omega/\omega_{,0.5}$ for five concentrations of ET-597 in three different-diameter tubes, obtaining a single curve. However, as the authors noted, some conceptual difficulties arise with regard to the definition of N_{Re} for the more concentrated solutions where pseudoplastic effects are present. Furthermore, as Equation (2) is now written, a value of β less than unity does not necessarily correspond to true drag reduction. Finally, we have the difficulty in evaluating $\omega_{,0.5}$ (corresponding to $\beta = 0.5$) for slightly drag-reducing systems.

These problems may be eliminated in the case of dilute